DEVELOPMENT OF MULTISPECTRAL ALGORITHM AND REMOTE SENSING TECHNIQUE FOR AIR QUALITY MEASUREMENTS OVER MAKKAH, MINA AND ARAFAH

By

NADZRI BIN OTHMAN

Thesis submitted in fulfillment of the requirements for the degree of Master of Science

JANUARY 2011

ACKNOWLEDGEMENTS

I first thank God Almighty for everything. Truly, all blessings come from Him.

I would like to thank my thesis supervisor, Assoc. Prof. Dr. Mohd Zubir Mat Jafri, for his guidance, assistance and encouragement throughout my graduate study. His scientific insight and perspectives have made working with him a rewarding and invaluable experience. I wish to thank him for giving suggestions in improving my project as well as the time spent for reviewing this report. I am particularly grateful to my co-supervisor Dr. Lim Hwee San for his help, support and sharing of information and thoughts throughout this project.

The friendship and assistance of the Remote Sensing Research Group, including Assoc. Prof. Dr. Khiruddin Abdullah, as well as friends at the School of Physics, has made my life at USM more enjoyable. My sincere thanks are due to Mr. Azmi Abdullah, Mr. Burhanuddin Wahi, Mr. Shahil Ahmad Khosaini and all the scientific and technical staff as well as my colleagues in the Engineering Physics laboratory.

I would like to acknowledge that the images and data used in this study were acquired using the United States Geological Survey (USGS) Global Visualization Viewer (GloVis), GES-DISC Interactive Online Visualization ANd aNalysis Infrastructure (Giovanni) as part of the NASA's Goddard Earth Sciences (GES) Data and Information Services Center (DISC).

The support from Ministry of Higher Education through Fundamental Research Grant Scheme IPTA (FRGS) (Grant No. 203/PFIZIK/6711107) and Universiti Sains Malaysia, through Research University Postgraduate Research Grant Scheme (USM-RU-PRGS) (Grant No. 1001/PFIZIK/831020).

Finally, yet importantly, I genuinely express my sincere gratitude to my parents, Othman bin Husin and Ruhamah binti Ithnin for their constant support and prayers throughout the course.

Nadzri

TABLE OF CONTENTS

LIST OF TABLES

LIST OF FIGURES

LIST OF ABBREVIATIONS

2D	Two dimension
3D	Three dimension
µm	Micrometre
A/D	Analog to Digital
AERONET	AErosol RObotic NETwork
Aexp	Angstrom exponent
ALOS	Advanced Land Observing Satellite
AOD	Aerosol Optical Depth
AOT	Aerosol Optical Thickness
APEX	Airborne Imaging Spectrometer
API	Air Pollution Index
ASD	Analytical Spectral Devices
ASTER	Advanced Spaceborne Thermal Emission and Reflection Radiometer
ATBD	Algorithm Theoretical Basis Document
atm	Atmosphere
ATCOR	ATmospheric CORrection
ATLID	ATmospheric LIDar
AVIRIS	Airborne Visible/Infrared Imaging Spectrometer
AVHRR	Advanced Very High Resolution Radiometer
BRDF	Bidirectional Reflectance Factor
C	Celsius
CALIPSO	Cloud Aerosol Lidar and Infrared Pathfinder Satellite Observation
cm	Centimetre
CO	Carbon Monoxide

DAACs	Earth Science Distributed Active Archive Centers
DDV	Dense Dark Vegetation
DEM	Digital Elevation Model
DN	Digital Number
DOE	Department of Environment
DTA	Differential Textural Analysis
ETM+	Enhanced Thematic Mapper Plus
EOS	Earth Observing System
F	Farenheight
FOV	Field-of-View
FWHM	Full-Width Half-Maximum
g	Gram
GCP	Ground Control Point
GIS	Geographic Information System
GPS	Global Positioning System
GOES	Geostationary Operational Environmental Satellites
GOME	Global Ozone Monitoring Experiment
Grescale	Rescaled gain
Brescale	Rescaled bias
IASI	Infrared Atmospheric Sounding Interferometer
IFOV	Instantaneous Field Of View
IKONOS	IKONOS Satellite
IRS	Indian Remote Sensing Satellite
JD	Julian Day
K	Kelvin
km	Kilometre

km/h	Kilometre per hour
Landsat	Land Satellite
LOWTRAN	Low Resolution Transmission
m	Metre
MERIS	MEdium Resolution Imaging Spectrometer
MISR	Multiangle Imaging SpectroRadiometer
MSS	Multispectral Scanner
mm	Millimetre
MODIS	Moderate Resolution Imaging Spectroradiometer
MODTRAN	MODerate spectral resolution atmospheric TRANsmittance algorithm
MOPITT	Measurements of Pollution in the Troposphere
NASA	National Aeronautics and Space Administration)
NIR	Near Infrared
NDVI	Normalized Difference Vegetation Index)
nm	Nanometer
NOAA	National Oceanic & Atmospheric Adminstration
NO_2	Nitrogen dioxide
O_3	Ozone
OMI	Ozone Monitoring Instrument
PM	Particulate Matter
PM1.0	Particulate Matter less than 1 micrometre in diameter
PM10	Particulate Matter less than 10 micrometre in diameter
PM2.5	Particulate Matter less than 2.5 micrometre in diameter
POLDER	POLarization and Directionality of the Earth's Reflectances
R	Correlation coefficient

RCR	Remote Cosine Receptor
RH	Relative Humidity
RMSE	Root Mean Square Error
RS3	Remote Sensing data acquisition and analysis software
RT	Radiative Transfer
SCIAMACHY	SCanning Imaging Absorption SpectroMeter for Atmospheric CartograpHY
SeaWiFS	Sea-viewing Wide Field-of-view Sensor
SLC	Scan Line Corrector
SMART	Simulated MISR Ancillary Radiative Transfer
SO_2	Sulphur dioxide
SPOT	Satellite Pour l'Observation de la Terre
sr	Steradian
TES	Tropospheric Emission Spectrometer
TIFF	Tagged Image File Format
TM	Thematic Mapper
TOA	Top of Atmosphere
TOMS	Total Ozone Mapping Spectrometer
USGS	United States Geological Survey
UTM	Universal Transverse Mercator System
UV	Ultraviolet
VIS	Visible
W	Watt
WHO	World Health Organization
WMO	World Meteorological Organization

LIST OF SYMBOLS

a	Algorithm coefficient
d	Earth-Sun distance
E_{SUN_λ}	Mean solar exo-atmospheric irradiances
F_o	Extraterrestrial solar flux
f(RH)	Ratio between these (size-distribution integrated) extinction efficiencies
H	AOT of the layer with height
I_λ	Solar irradiance reached the ground at wavelength, λ
$I_{o\lambda}$	Solar irradiance at the top of atmosphere at wavelength, λ
K_{scat}	Extinction coefficient due to scattering by aerosols
K_1	Calibration constant (666.09 $Wm^{-2}sr^{-1}\mu m^{-1}$)
K_2	Calibration constant (1282.71 Kelvin)
L_{TOA}	Radiance at TOA
L_λ	Spectral radiance
L_{MIN_λ}	Spectral radiance that is scaled to Q_{CALMIN}
L_{MAX_λ}	Spectral radiance that is scaled to Q_{CALMax}
M	Relative optical mass
n(r)	Aerosol size distribution under dry conditions
$n_{amb}(r)$	Size distribution under ambient relative humidity conditions
θ_s	Solar zenith angle
θ_v	Viewing zenith angle
ρ_p	Unitless planetary reflectance

ρ_a	Path radiance/reflectance due to aerosol or Mie scattering
ρ_m	Path radiance due to molecular or Rayleigh scattering
ρ_{TOA}	Top of atmosphere path radiance/reflectance at satellite level
ρ_{atm}	Atmospheric reflectance/path radiance
ρ_{ground}	Reflectance at a surface target (= albedo for Lambertian)
P	Phase function
P_a	Aerosol scattering phase function
P_m	Molecular scattering phase function
Q_{CAL}	Quantized calibrated pixel value in DN
Q_{CALMIN}	minimum quantised calibrated pixel value (corresponding to L_{MIN_λ}) in DN
Q_{CALMax}	maximum quantised calibrated pixel value (corresponding to L_{MAX_λ}) in DN
$Q_{ext,amb}$	Extinction efficiency under ambient conditions
$Q_{ext,dry}$	Extinction efficiency under dry conditions
$\langle Q_{ext} \rangle$	Size-distribution integrated extinction efficiency
R_λ	Atmospheric reflectance corresponding to wavelength for satellite
r	Radius
r_{eff}	Effective radius
T_λ	Atmospheric transmittance at certain wavelength
S_{albedo}	Atmosphere spherical albedo from below
T_{atm}	Atmospheric transmissions
$T(\theta_s)$	Ability of the atmosphere to transmit radiant flux from the sun to

	the target
$T(\theta_v)$	Ability of the atmosphere to transmit radiant flux from the target to the sensor system
T	Effective at-satellite temperature in Kelvin
τ	Optical depth or optical thickness
τ_λ	Total atmospheric optical thickness at certain wavelength
τ_a	Attenuating coefficients which are made up primarily of aerosol or particle (Mie scattering)
τ_m	Attenuating coefficients which are made up primarily of molecule (Rayleigh scattering)
μ	Cosines of the view directions
μ_o	Cosines of the illumination directions
π	Pi (approximately equal to 3.14159265)
ω_o	Single scattering albedo
x	Particle diameter in micrometre
z	Ground to the satellite
$\propto$	Proportional to
λ	Wavelength
%	Percentage
$\pm$	Plus minus
~	Approximately

PEMBANGUNAN ALGORITMA MULTISPEKTRUM DAN TEKNIK PENDERIAAN JAUH UNTUK PENGUKURAN KUALITI UDARA DI MAKKAH, MINA DAN ARAFAH

ABSTRAK

Penganggaran penunjuk kualiti udara daripada pengukuran satelit dikenali sebagai muatan patikel atmosfera, yang diukur berdasarkan ketebalan optik lajur serakan aerosol. Akibat yang dibawa oleh pencemaran patikel ini menarik minat ramai penyelidik untuk melakukan kajian tentang erosol dan juga patikel bahan. Kajian ini membincangkan tentang potensi pengukuran kepekatan patikel bersaiz kurang daripada 10 mikrometer (PM10) dan ketebalan optik erosol (AOT) yang terkandung dalam atmosfera menggunakan imej satelit Landsat 7 ETM+ di kawasan Makkah, Mina dan Arafah. Algoritma multispektrum dibangunkan dengan menganggap keadaan permukaan kawasan kajian adalah lambertian dan homogen. Ia juga mengabaikan kesan atmosfera yang disebabkan oleh serakan Rayleigh. PM10 diukur dengan menggunakan meter habuk model 8520, manakala data AOT diukur dengan menggunakan spektroradiometer bimbit FieldSpec dan lokasinya ditentukan dengan menggunakan sistem penentududukan sejagat (GPS) bimbit. Hukum Beer Lambert digunakan untuk mengira AOT daripada pancaran atmosfera yang diukur dengan menggunakan spektroradiometer bimbit FieldSpec. Nombor digital (DN) yang direkodkan oleh satelit pengimejan ditukarkan kepada kepantulan atasan atmosfera (TOA), iaitu jumlah kepantulan permukaan dengan kepantulan atmosfera. Seterusnya, kaedah pembetulan atmosfera (ATCOR2) digunakan untuk menerbitkan nilai kepantulan permukaan. Kepantulan atmosfera diperoleh dengan menolakkan nilai kepantulan atasan atmosfera (TOA) dengan kepantulan permukaan. PM10 dan AOT yang diukur dikorelasikan dengan nilai kepantulan atmosfera menggunakan

teknik regresi. Pelbagai jenis algoritma regresi diuji dengan membandingkan nilai pekali korelasi (R) dan nilai sisihan punca min kuasa dua (RMSE). Seterusnya, algoritma regresi tiga jalur (Merah, Hijau dan Biru) dengan nilai R tertinggi dan RMSE terendah dipilih untuk menghasilkan peta PM10 dan AOT bagi kawasan kajian. Pelbagai jenis penuras dan saiz tetingkap digunakan seperti purata, median dan mod telah dikenakan ke atas imej satelit Landsat 7 ETM+ bagi menambah ketepatan dan mengurangkan kesan hingar terhadap peta PM10 dan AOT di kawasan kajian. Model algoritma multispektrum menunjukkan bahawa PM10 dan AOT yang tinggi semasa musim haji berbanding dengan musim yang lain. Keputusan keseluruhan untuk nilai dihitung bagi PM10 mempunyai ketepatan purata masing-masing 0.897 ± 0.085 $\mu g/m^3$ dan 0.870 ± 0.095 $\mu g/m^3$ untuk hari tunggal dan gabungan tiga hari. Manakala, nilai AOT yang dihitung memberikan ketepatan purata 0.8775 ± 0.0676. Algoritma AOT yang dicadangkan juga disahkan dengan menggunakan data pelbagai tarikh dan produk aerosol daripada Terra Moderate Resolution Imaging Spectroradiometer (MODIS) dan Multiangle Imaging SpectroRadiometer (MISR) berada dalam lingkungan ± 5% daripada nilai yang dikira. Keputusan ini memberikan keyakinan bahawa algoritma multispektrum AOT dan PM10 dapat membuat ramalan yang tepat terhadap konsentrasi AOT dan PM10 di kawasan kajian.

DEVELOPMENT OF MULTISPECTRAL ALGORITHM AND REMOTE SENSING TECHNIQUE FOR AIR QUALITY MEASUREMENTS OVER MAKKAH, MINA AND ARAFAH

ABSTRACT

The air quality indicator approximated by satellite measurements is known as an atmospheric particulate loading, which is evaluated in terms of the columnar optical thickness of aerosol scattering. The effect brought by particulate pollution has gained interest among researchers to study aerosol and particulate matter. This study presents the potentiality of retrieving concentrations of particles with diameters less than ten micrometre (PM10) and aerosol optical thickness (AOT) in the atmosphere using the Landsat 7 ETM+ satellite imageries over Makkah, Mina and Arafah. A multispectral algorithm was developed by assuming that surface condition of the study area was lambertian and homogeneous. It also neglected atmospheric effect due to Rayleigh scattering. PM10 in situ measurements were collected using DustTrak aerosol monitor 8520, while AOT data was measured using FieldSpec handheld spectroradiometer and their locations were determined by a handheld global positioning system (GPS). The Beer Lambert law was used to calculate AOT from transmittance of atmospheric measured using the FieldSpec handheld spectroradiometer. The digital number (DN) recorded by satellite imageries were converted to top of the atmosphere (TOA) reflectance, which is the sum of the ground reflectance and atmospheric reflectance. Then, the atmospheric correction (ATCOR2) method was used to retrieve the surface reflectance. Atmospheric reflectance is obtained by subtracting the reflectance at the top of the atmosphere (TOA) with the surface reflectance. Measured PM10 and AOT were correlated with atmospheric reflectance value using regression technique. Various types of

regression algorithms were then examined by comparing the correlation coefficient (R) values and the root-mean-square error (RMSE) values. Then, the three band regression algorithm (Red, Green and Blue) with highest R value and the lowest RMSE was selected to generate PM10 and AOT maps for the study areas. Various types of filters and windows size were used, for example, average, median and mode, were applied to Landsat 7 ETM+ satellite imageries in order to increase the accuracy and to minimise the noise effect of the PM10 and AOT maps over the study area. The multispectral algorithm model showed that PM10 and AOT were high during Hajj season as compared to other season. The overall results for calculated values of PM10 had average accuracy of 0.897 ± 0.085 $\mu g/m^3$ and 0.870 ± 0.095 $\mu g/m^3$ for single day and combined three days respectively. While calculated values of AOT gave average accuracy of 0.8775 ± 0.0676. The proposed AOT algorithm was also validated using multi temporal data and aerosol product from the Terra Moderate Resolution Imaging Spectroradiometer (MODIS) and the Multiangle Imaging SpectroRadiometer (MISR), and were within ±5% of calculated values. These results provide confidence that the multispectral algorithm AOT and PM10 models can make accurate predictions of the concentrations of AOT and PM10 over the study area.

CHAPTER 1

INTRODUCTION AND OVERVIEW

1.1 Research Background

Air pollution is currently one of the major problems in developed countries as well as developing countries. Air pollution concentrations are the result of interactions among local weather patterns, atmospheric circulation features, wind, topography, human activities, human responses to weather changes, and other factors. The contributing factors to air pollution include increasing use of motor vehicles, forest burning and desert dust. Air pollution occurs when the concentration of polluting gases, substances and particles in the atmosphere exceeds the specified safety levels.

The five pollutants, ozone (O_3), nitrogen oxide (NO_2), carbon monoxide (CO), sulphur dioxide (SO_2) and particulate matter (PM) are referred to as criteria of the air pollution index (API) by the Department of Environment (DOE) Malaysia. Generally, the amounts of O_3, NO_2, CO, SO_2, PM10, temperature, humidity, wind direction and speed are measured at ground stations.

Air pollution causes illnesses, deaths and respiratory diseases such as asthma (Pope et al., 1995). Medical studies tend to demonstrate that breathing diseases or asthma may be linked to high value of pollutants and most affected people suffering from respiratory conditions such as asthma; both the very young and old, and people living in poverty are particularly at risk (Wald and Baleynaud, 1999; Brauer et al., 2001). Wheezing, coughing and eyes watering are the preliminary symptoms experienced by the sensitive group, which lead to constant breathing problems, persistent pain in the chest and skin irritations.

Aerosols are a subset of air pollution that refers to the tiny particles varying from 0.001 μm to 100 μm in diameter (d), as in Figure 1.1. The aerosol size, distribution and composition are widely variable and depend on their different sources. Primary aerosols are emitted directly as particles and secondary aerosols are formed in the atmosphere by gas to particle conversion processes.

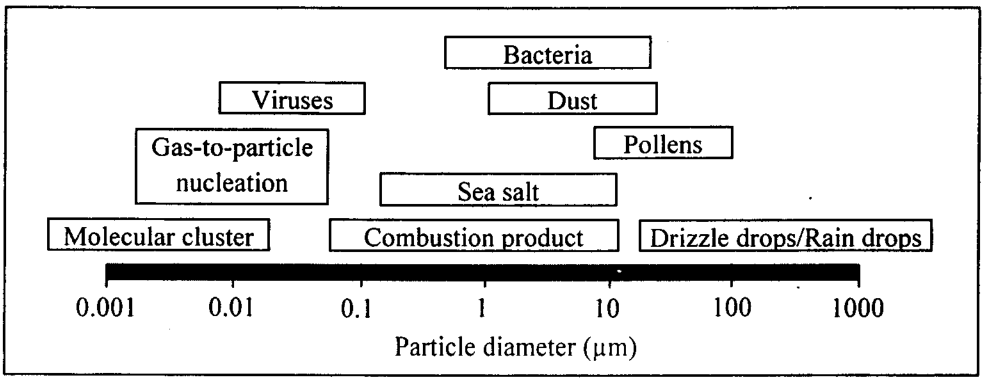

Figure 1.1: Description of aerosols particle diameter in micrometre (modified from Morawska, 1999)

Aerosols are classified into three modes according to their sizes: nucleation (d < 0.1 μm), accumulation (0.1 < d < 1 μm) and coarse (d > 1 μm). The aerosol size distribution has been fitted with various distributions, such as power low, gamma and log-normal distributions (Warneck, 1999).

The residence time of aerosols depends on their size, chemistry and height in the atmosphere. Particle residence times range from minutes to hundreds of days. Aerosols between 0.1 μm - 1.0 μm (the accumulation mode) remain in the atmosphere longer than the other two size categories. Due to the short aerosol lifetimes (days or weeks), it can change in visibility and radiative forcing in different parts of the globe due to aerosols distribution over the particular area.

PM is a general term used for aerosols, small liquid droplets, or solid particles that are found in air. These are much larger than individual molecules. The EPA uses the abbreviations PM2.5 and PM10 to specify particulate matter less than 2.5 μm and between 2.5 μm 10 μm, respectively. In some areas PM can be very heavy because of high levels of industrial activity or natural environmental conditions from a variety of sources, such as vehicles, factories, construction sites, farming, unpaved roads, burning wood, and blowing sand and dust in desert environments. In these types of environments, larger amounts of PM can be inhaled. PM10 or smaller acts to increase the number of respiratory diseases, especially in regard to cardio-vascular illnesses and reduced visibility by their scattering and absorption of radiation (Husar et al., 1981; Ball and Robinson, 1982).

Air quality monitoring at urban and regional scales has traditionally been done using a network of ground monitoring stations combined with dispersion models that predict air quality between monitor locations (Bozyazi, 1998; Chakraborty et al., 1999; Kassteele, 2006). Such monitoring programmes required a high maintenance and implementation costs and also are limited in spatial coverage (Builtjes et al., 2001; Ung et al., 2001). Satellite remote sensing can provide a synoptic picture of air quality in a regional air shed, including information about sources and source locations for isolated events. Satellite sensors can provide a broad view of urban haze and help determine when there is impact on urban air quality by local fires, dust storms, or trans-boundary transport of pollutants from more distant sources. These sensors can potentially be used to monitor air quality in rural or remote regions with no ground-based monitoring network.

In earlier work, it has been shown that satellite data and imagery can be applied to air quality policy. Different methods for the image-based retrieval and spatial mapping of aerosol parameters have been developed using remote sensing technique. Satellite imagery can be used to assess the spatial structure of air pollution and interactions on global, regional, or local dispersion patterns better.

1.2 Hajj Pilgrimage and its Relationship with Air Pollution

Air pollution has become an increasingly important environmental issue in the Middle East. High levels of suspended particulates have become a common parameter of many regions. Emissions of SO_2 have been rising steadily as industrialisation occurs. Other gases like NO_2 and CO have also been increasing steadily in many localities.

Saudi Arabia is located in a dry area where precipitation rarely occurs and surface winds are inactive almost all the year round. In Saudi Arabia, dust plays a primary role in causing air pollution in a country which is 90 % desert. The desert is the source region of dust (Presidency of Meteorology and Environment (PME), 2007) and is characterised by periodical outbreaks of dust storms that transport large amounts of desert dust in the troposphere, resulting in enhanced optical thickness value that is correlated with the aerosol direct radiative forcing.

The higher rates of air pollution in Saudi Arabia are strongly correlated with the economic progress growth witnessed over the past three decades. Therefore, the Kingdom of Saudi Arabia has paid special attention to monitoring and reducing such emissions through concerted efforts undertaken at both national and international levels.

The rapid development of the Kingdom, particularly in urban areas, has been accompanied by a deterioration of air quality as a direct consequence of the massive increase in land transportation (i.e. cars, trucks and buses) and the associated growth in the emission of air pollutants. In addition to these mobile sources of air pollution, there has been the growth in stationary sources of air pollution, such as factories, desalination plants, power stations and oil refineries. Air pollutants generated by these sources depend on the quality and mix of fuel used and its efficiency, as well as the level of technology, design efficiency and operating cycles.

Each year, millions of pilgrims arrive in the Holy City of Makkah during Hajj season beginning 8th Dzulhijjah to 12th Dzulhijjah. It is noted that the number of pilgrims coming from outside the kingdom had increased since 1350 H, the number of pilgrims did not exceed one hundred thousand pilgrims until the year 1369 H. In the year 1999, 1,831,998 pilgrims performed the Hajj including 1,056,730 international travellers from over 140 countries and 775,268 domestic pilgrims as shown in Table 1.1. The year 2006 saw a total of 2,130,594 pilgrims arriving in the Kingdom, with international and domestic travellers numbering 1,557,447 and 573,147, respectively. The annual increase of pilgrims until 1429 H amounted to 1,729,841 pilgrims from abroad, while the domestic pilgrims residing in the Kingdom numbered 679,008 pilgrims, to make 2,408,849 pilgrims in 1429 H. The number of Umrah performers in 1430 H increased to 300 thousand as compared to 1429 H. This mass migration (Figure 1.2) entails some of the world's most important public-health and infection control problems.

Table 1.1: Numbers of Hajj pilgrims (1999 - 2006)

Year	Saudis	Non-Saudis	Total
1419/1999	775,268	1,056,730	1,831,998
1420/2000	571,599	1,267,555	1,839,154
1421/2001	549,271	1,363,992	1,913,263
1422/2002	590,576	1,354,184	1,944,760
1423/2003	610,117	1,431,012	2,041,129
1424/2004	592,368	1,419,706	2,012,074
1425/2005	629,710	1,534,769	2,164,469
1426/2006	573,147	1,557,447	2,130,594

(Source: Hajj and Umrah Statistics, Ministry of Hajj Kingdom of Saudi Arabia, 2009)

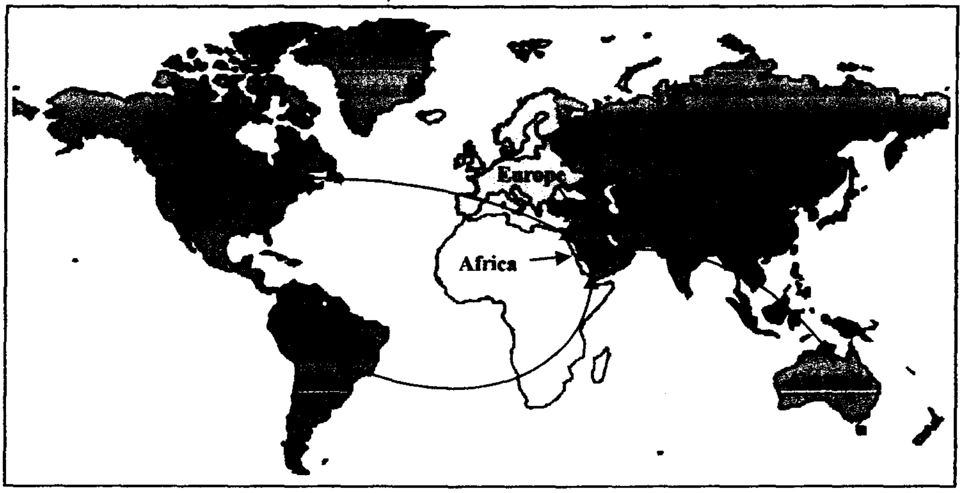

Figure 1.2: Numbers of pilgrims arriving for the Hajj from abroad (modified from Ahmed et al., 2006)

Increasing pilgrim numbers is accompanied by increased daily activities including the demands for transportation. Consequently, considerable quantities of gaseous and solid pollutants are emitted to the atmosphere. The emitted pollutants could cause many harmful environmental impacts to the Holy City of Makkah and nearby places.

Some studies on air pollution conducted in the Holy City of Makkah, Saudi Arabia, focused on the central area near the Holy Mosque and on the Holy places (Mina and Arafah). These studies showed that there are high concentrations of air pollutants in the atmosphere, exceeding the standards that are attributed to traffic emission during the Hajj season, where about three million people gathered in these limited areas (Al-Amri and Abu-Alghat, 1992; Badwi and Al-Hosary, 1993; Al-Thumali, 1998; Yacob, 2000; Al-Jeelani and Ramadhan, 2004; Al-Jeelani, 2009). There are many studies assessing the air quality inside the tunnels near the Holy Mosque, which showed that there were very high concentrations of PM10 that violated the standards of API (Al-Sawas, 1995; Al-Raddadi, 1996; Al-Jeelani, 2009).

1.3 Literature Review on the Application of Remote Sensing in Air Pollution Studies

Spaceborne remote sensing instruments have provided the earth sciences with a wealth of information in recent decades. The first earth observation satellite was the Television InfraRed Observation Satellite-1 (TIROS-1), a weather satellite launched April 1960 by the National Aeronautics and Space Administration (NASA), part of the TIROS programme and eventually superseded by the satellite series operated by the National Oceanic and Atmospheric Administration (NOAA) (Rees, 2001). Scientific and operational earth observation satellites carry a variety of passive and active instruments operating in wavelength regions ranging from microwaves to UV and in geometries ranging from limb to nadir observation.

Aerosols and gasses in the atmosphere disturb the radiance reaching to the sensor by scattering and absorption. This reduces the contrast of the remotely sensed images (Sifakis et al., 1998). Optical thickness indicates the amount of scattering and absorption by particles and gasses. The optical characteristics of atmospheric aerosol are needed in order to derive the AOT and mass burden from path radiance measurements taken from space (Fraser et al., 1984; Kaufman and Sendra, 1988; Holben et al., 1992; Martonchik and Diner, 1992), or the aerosol single-scattering albedo (Kaufman, 1987) and the particle size (Kaufman et al., 1990). The first applications of satellite remote sensing of aerosols began in the mid-1970s and concerned the detection of desert particles above the ocean (Fraser, 1976; Griggs, 1979; Norton et al., 1980). Fraser (1976), Norton et al. (1980) and Griggs (1979) used land observing satellite (Landsat), Geostationary Operational Environmental Satellites (GOES), and Advanced Very High Resolution Radiometer (AVHRR) data, respectively.

MODIS measures aerosol optical thickness over land with an estimated error of ± 0.05 to ± 0.20 (Kaufman et al., 2002). The spatial resolution of SCanning Imaging Absorption SpectroMeter for Atmospheric CartograpHY (SCIAMACHY) and Ozone Monitoring Instrument (OMI) are largely improved compared to GOME-1 and allow particular pollution patterns on regional scales to be resolved. Sensors for monitoring aerosols are the Advanced Along Track Scanning Radiometer (AATSR) on board Envisat, and its pre-decessors, the Along Track Scanning Radiometers (ATSR-1 and -2), on board ERS-1 and -2 which provide column-integrated data at coarse resolution (Builtjes et al., 2001). Moderate Resolution Imaging Spectroradiometer MODIS and Multi-angle Imaging SpectroRadiometer (MISR) are sensors at Terra satellite used to detect climate change by aerosols (NASA, 2002). All these instruments have low to medium spatial resolution.

AOT also can be calculated from multi-spectral images with higher resolution, such as Landsat ETM+. Crist et al. (1986) described the method to normalise Landsat data affected by haze, using the third feature of the Tasseled Cap transformation. This study showed that atmospheric scattering decreased in severity with increasing wavelength, and since the visible bands of the Landsat Multispectral Scanner (MSS) sensor (i.e. band 1 and band 2) were highly correlated in their response to surface features, a contrast of these two bands, as represented in yellowness, could be expected to provide atmospheric scattering information. The method developed by Tanre et al. (1988) which allowed deriving AOT over land surfaces from satellite data by using the blurring effect due to scattering by assuming the ground reflectance to be constant, variations of the satellite signals may be attributed to variations of the atmospheric optical properties. The method was applied to Saharan aerosols, which represented the most important contribution to the atmospheric aerosol loading. The result derived from the Thematic Mapper (TM) data proved to be in good agreement with simultaneous ground-based measurements. The determination of AOT from the atmospheric transmission is based on the ratio of transmission between several images and it is known as the contrast reduction. Tanre et al. (1988) suggested and applied the method of TM images taken over arid region. The variation in the transmission is determined from the variation of the difference between the radiance from pixels located at a specified distance apart. The information of some major satellite remote sensing applicable for tropospheric aerosol studies is listed in Table 1.2.

Table 1.2: Present remote sensing satellite applicable for remote sensing troposphere aerosol

Instruments	Sensor	Parameters measured
UV-VIS-NIR spectrometers	OMI, SCIAMACHY, GOME, GOME-2	O_3, NO_2, SO_2, Formaldehyde, Glyoxal, CO, CH_4, Absorbing aerosols
VIS-NIR Radiometers	AVHRR, MODIS, MISR, MERIS, (A)ATSR(-2), POLDER	Aerosol parameters: optical thickness and fine/coarse fraction
TIR Spectrometers	MOPITT, IASI, TES	Ozone profiles, CO
Active Instruments	CALIPSO, ATLID	Aerosol profiles
Mid-Resolution Optical instruments	Landsat 5 TM, Landsat 7 ETM+, SPOT	AOT over oceans; AOT of dust over land using contrast effect.

(Source: King et al., 1999)

Satellite instruments provide global coverage with high spatial resolution, relatively low temporal resolution and allow moderately accurate retrievals. Ground-based instruments have limited spatial coverage, relatively high temporal resolution (many measurements per day), and are generally regarded as more accurate retrievals. As a result, ground-based instruments, such as a narrow band sun photometer (Schaap et al., 2008) and spectroradiometer (Brogniez et al., 2008) are often used for validation of satellite based retrievals. Therefore, these equipments are able to collect values of the AOT in the same wavelength bands of the satellite imagery. Those permanent narrow band sun photometer and spectroradiometer used widely is AErosol RObotic NETwork (AERONET) (Holben et al., 1998) and RSS-1024 Rotating Shadowband Spectroradiometer (Harrison et al., 1999), respectively. The equipment, such as MICROTOPS II hand-held sunphotometer and FieldSpec handheld spectroradiometer, come in handy as they are mobile and able to collect the optical readings anywhere (Lim, 2006).

Uncertainty and variability in the aerosol size distribution and corresponding scattering phase function generates major errors in the derived aerosol optical thickness over the desert (Kaufman and Sendra, 1988). The dust particles are large (effective radius m), and the desert is not vegetated. Algorithms that use other parts of the spectrum, such as the ultraviolet (Hsu et al., 2004) help to overcome the problems in determining aerosol over bright desert, the magnitude of dust absorption is determined if dust has brightens or darkens the image. This property is very useful to estimate the AOT. Such satellite measurements, in agreement with in situ, aircraft and radiation network measure of dust absorption, helped to solve a long standing uncertainty in desert dust absorption of sunlight. Kaufman et al. (2000) succeeded in using the combination of the desert brightness at 2.1 m with dust-light absorption and some unknown mechanism that keeps the ratio of the spectral surface reflectance at roughly 0.5 or 0.25 between the red or blue channels to the 2.1 m channel, respectively, independent of the surface cover.

The strength of linear relationship between satellite-made observations and air quality parameters using low and medium spatial spectral resolution of satellite bands had been investigated by many researchers for the past few years. For example, Ahmad and Hashim (2002) showed the relationships between ground-truth measurements of haze API and satellite recorded atmospheric reflectance/path radiance of bands 1 and 2 to quantify haze components from NOAA-14 AVHRR data and map their spatial distribution based on local API index of the individual haze components of PM10, CO, SO_2, NO_2 and O_3 using regression models. More recently, Lim (2006) investigated the use of two bands regression algorithm correlated with atmospheric reflectance (bands 1 and 3 of Landsat 5 TM and 7ETM+) to determine AOT and PM10 concentration map over Penang Island using dark target and ATCOR2 technique. ATmospheric CORrection (ATCOR) module, developed by Dr. Rudolf Richter (Richter, 1996a, 1996b, 1997, 2005; Ricther et al., 2009), has been used widely to determine the surface reflectance for satellite image. Kneubuhler et al. (2005) used ATCOR2 to correct data from optical spaceborne sensors, atmospherically, assuming flat terrain conditions and ATCOR3 accounts for terrain effects by incorporating digital elevation model (DEM) data and their derivatives such as slope surface. Many researchers have documented that there is a strong correlation between the AOT and PM10 data (Chu et al., 2002; Wang and Christopher, 2003). Sifakis et al. (2002) studied the potentiality of using NOAA-15 observations for obtaining AOT maps over the metropolitan area of Athens through Differential Textural Analysis (DTA) algorithm. The correlation coefficient (R) as high as 0.78 to 0.95 had been obtained between the AOT and the PM10 measurements.

A methodology was developed using the satellite imagery of atmospheric aerosol and land surface features that allows us to locate and characterise the sources of pollutants. The sources of the dust events were located and their land surface was characterised. Earth observation satellites record data in different spectral bands or wavelength intervals. With these spectral bands it is possible to construct different band combinations into false colour images or via the implementation of various algorithms that operate on one or more of those bands to correlate with in situ AOT and PM10 ground truth data.

1.4 Problem Statement

The aerosol and PM have been increasing steadily in many localities. Dust aerosols, which are prevalent over the desert, can be transported to downwind areas thousands of kilometres away from source regions, degrading visibility and air quality, perturbing the radiative transfer in the atmosphere, providing a vector for disease causing organisms, and exacerbating symptoms in people with asthma (Prospero, 1999).

Over two million pilgrims converge every year at the same time to perform this religious duty (Yacob, 2000; Al-Jeelani and Ramadhan, 2004; Al-Jeelani, 2009). The result is a crowded event of extraordinary magnitude leading to uniquely challenging problems. One of the challenging problems during the Hajj is the air quality problem that introduces many difficulties among pilgrims and authorities in term of health and other problems.

Present satellite remote sensing products only provide the air quality measurement in a large area. This reduced the accuracy of the distribution of air quality. In general, a limited number of ground data collection locations are available, because ground data collection is expensive (Ung et al., 2001). With a limited number of data collection points, the use of mathematical models and interpolation methods only, do not give a correct picture of the air pollution for any given area. By using the remote sensing technique, the satellite image together with ground truth data, AOT and PM10 concentrations are measured frequently by the multi-temporal date, could generate valuable information on aspects related to air pollution at specific scale of the study area more accurately.

1.5 Objectives

The objectives of this study are as follows:

1. To develop an algorithm for air quality measurements over semi arid area of Makkah, Mina and Arafah.
2. To calibrate the developed algorithm for remote sensing air quality mapping.
3. To validate the results using ground truth data and other satellite data.

1.6 Scope of the Study

The major effect of the atmospheric aerosol on space observations is through the path radiance (Kaufman, 1993). The algorithm presented in this study is based on the relationship between the spectral path radiance (radiance that contaminates satellite observations of the Earth) and the aerosol optical thickness using analytical derivations based on single-scattering radiative transfer theory.

Then, this technique was applied to the three sets of multi-temporal Landsat 7 ETM+ data, initially for solar zenith angles of 45 to 52 degree in order to be able to monitor dust events, sources, transport and to minimise the solar zenith effect. Landsat 7 ETM+ satellite data set was selected due to the availability of the corresponding ground truth measurements of the AOT and PM10.

The algorithm validation was performed using in situ data and AOT product of Terra MODIS and MISR satellite. The advantage of the technique over the visible band is that, it is equally sensitive to dust in the entire vertical column. However, the technique is very sensitive to dust absorption. In the red and green part of the spectrum, dust from the desert is weak-absorbing or non-absorbing, and therefore, the technique is best applied in this channel. In the blue part of the spectrum, the dust absorption and the uncertainty in it makes the technique less successful.

1.7 Significance of the Study - The Importance and the Benefits of the Research

The research will contribute a model of a multispectral algorithm to predict and observe the trend of the air quality distribution in Makkah, Mina and Arafah areas. The next stage of the study will focus on finding solutions for the improvement of the current problems. Research outputs will be supplied to relevant Saudi Arabian authorities. Besides, the outputs will also benefit the Saudi Arabian Government for establishing an efficient system for mapping and monitoring the air quality. Also, Hajj pilgrims will be well informed of the air quality levels at the ritual locations, thus ensuring an easy and smooth process in performing the Hajj rituals.

1.8 Structure of the Thesis

The thesis starts with the introduction and overview chapter which gives an insight to the air quality remote sensing and its benefits. The objectives and the research questions to be answered in the present study are also presented in this chapter.

The second chapter gives a brief account of the study area, research materials and methodology that have gone through the research phase. The third chapter explains the theory of the algorithm development, which, in general, covers the theory of the optical remote sensing concept and radiative transfer that are used for developing the new algorithm of air quality remote sensing. A new algorithm that relates the atmospheric path radiance/reflectance to PM10 and AOT ground truth data is discussed.

The fourth chapter consists of the calibration and analysis of developed algorithm applying on satellite images using PM10 ground truth data. This chapter also consists of the discussion for all the data used and followed by a conclusion. The fifth chapter calibrates and analyses the developed algorithm applying on satellite images using AOT ground truth data. The AOT is calculated using Bouguer–Lambert law formula. Chapters Four and Five use the multi-temporal satellite data to see the suitability of the algorithm.

The sixth chapter shows the validation of the results from the PM10 and AOT algorithm using ground truth data. The correlation between the AOT and the PM10 is established in this chapter. The availability and correlation of the AOT data using the AOT product of Terra MODIS and MISR satellite sensor of AOT product over the study area are discussed.

Chapter Seven summarises all the outputs and results from the study. Recommendations for future study are also included in this chapter.

CHAPTER 2

STUDY AREA, RESEARCH MATERIALS AND METHODOLOGY

2.1 Introduction

In this chapter, the study area, research materials and methodology involved in this research are described. In addition, processing steps involving all the datasets used in the research work for the thesis are also described.

2.2 Study Area

Saudi Arabia (Figure 2.1) is located in the Middle East, and borders with the Persian Gulf and the Red Sea. The capital city is Riyadh, and the Kingdom is split into thirteen provinces. Currently, the population of the Kingdom is just over 27,136,977, which includes around 8,429,401 non nationals (Gulf Research Center, 2010). The Kingdom of Saudi Arabia occupies four-fifths of the Arabian Peninsula, with a land area of about 2,000,000 km^2 (900,000 m^2), (Memish et al., 2010). In Saudi Arabia, the government is headed by the monarchy, and the present King and Prime Minister is King Abdullah. Located in the southwest corner of Asia, the Kingdom is at the crossroads of Europe, Asia and Africa. It is surrounded by the Red Sea in the West, by Yemen and Oman in the South, the Arabian Gulf and the United Arab Emirates and Qatar in the East, and Jordan, Iraq and Kuwait in the North. Saudi Arabia's Red Sea coastline stretches about 1,760 kilometres, while its Arabian Gulf coastline is roughly 560 kilometres.

Since 1986, large scale public works to expand the places of worship central to the Hajj, (costing estimated US$22.5 million) have been carried out by royal decree

(Memish et al., 2003). As a result, each mosque at Makkah and Madinah can welcome 0.8 million pilgrims at one time.

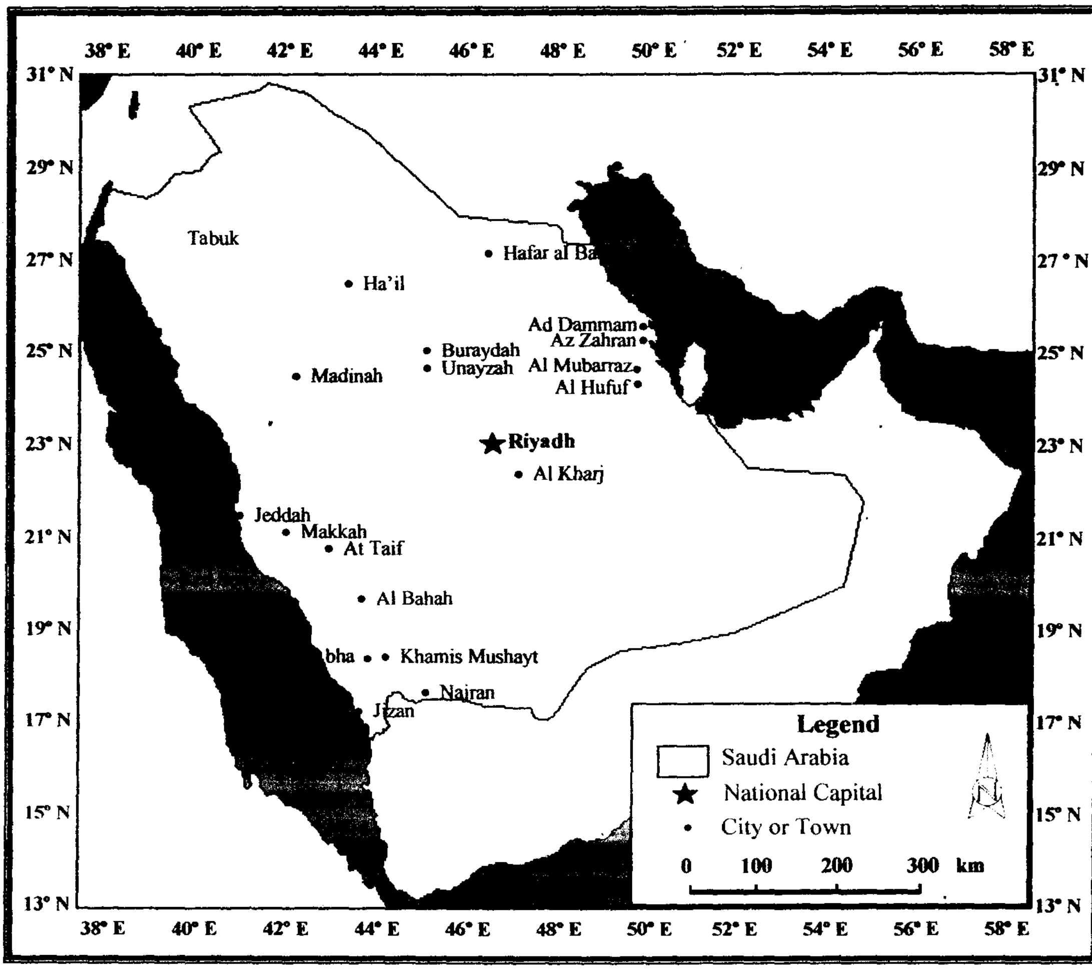

Figure 2.1: Map of Saudi Arabia (modified from: Saudi Geological Survey, 2008)

The Holy City of Makkah (Latitude 21°25'19" North Meridian 39°49'46") is at an elevation of 277 m above sea level, and approximately 80 km inland from the Red Sea (Figure 2.2). The elevations of Makkah Al Mukarramah are a group of mountains and black rocky masses which are granitic basement rocks (Al-Jeelani, 2009). Mountains are traversed by a group of valleys, such as the Ibrahim Valley. The Kaabah's location is in this valley.

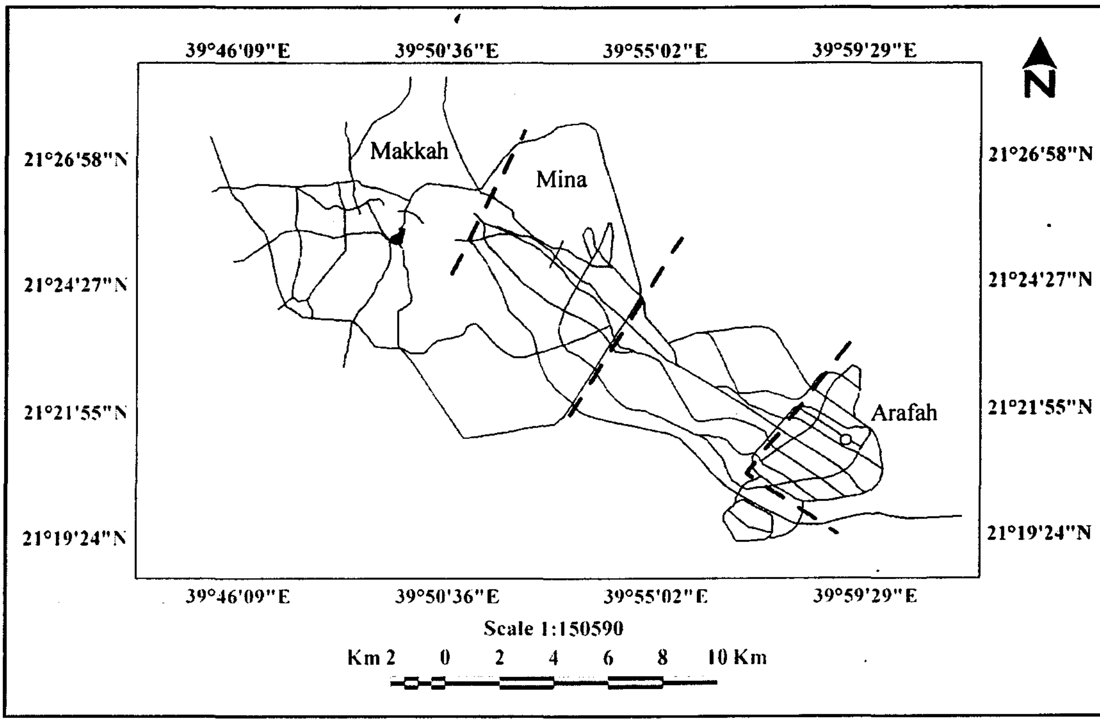

Figure 2.2: Locations of Makkah, Mina and Arafah

Mina is the place of encampment during the Hajj. The departure to Mina is normally from near the Haram, and the standard transportation mode is air conditioned buses, although thousands walk. Usually there is no time constraint. However, the combined effects of overcrowding tension, temperature, and pollution can be dangerously overwhelming for the vulnerable.

Arafah is about 4 km from Mina. Again because of heavy traffic it may take several hours to travel that distance to Arafah. The weather in Arafah is dry and hot (Al-Jeelani, 2009). The night in Muzdalifah usually passes quickly under the open sky. Adverse weather changes are uncommon. Coolness can come as a surprise blessing, but this rarely happens.

Makkah climate is different from other Saudi Arabian cities, retains its warm temperature in winter (November to Mac), which can range from 17 °C at midnight to 25 °C in the afternoon. During summer (April to October), temperatures are considered very hot and break the 40 °C mark in the afternoon dropping to 30 °C in the evening. Rain is very rare, with an average of 10-33 mm, and usually falls in December and January; the humidity is about 45-53 %. Winds are north-eastern most of the year. This region also faces with some natural events that often happen during the year, such as dust storms in summer, coming from the Arabian Peninsula's deserts or from North Africa (Al-Jeelani, 2009).

2.3 Research Equipment

2.3.1 ASD FieldSpec Handheld Spectroradiometer

ASD's FieldSpec handheld is a 512 element photodiode array spectroradiometer with a 325-1075 nm wavelength range, 1.5 nm sampling (bandwidth), 3.5 nm resolution and scan times as short as 17 ms. The built-in shutter, DriftLock dark current compensation and second-order sorting filter provide one with data that is free from errors often associated with other low cost instruments. With ASD's RS3 software one can easily measure and view reflectance, transmission, radiance, or irradiance spectra in real-time.

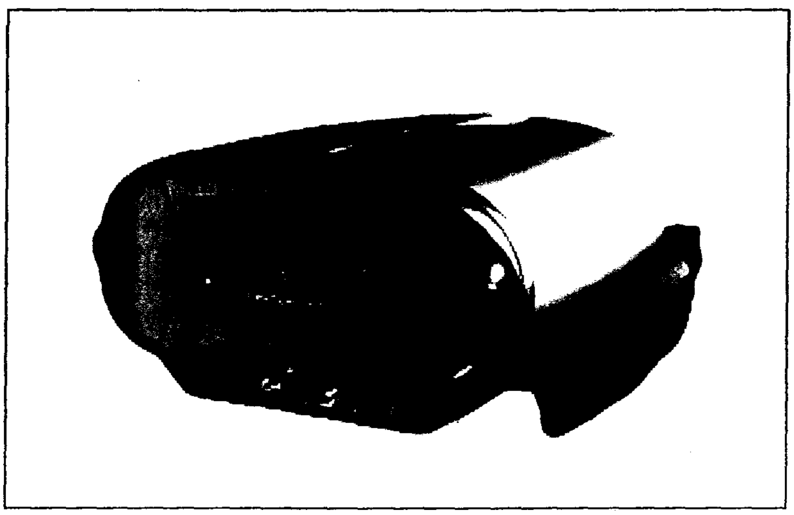

Figure 2.3: ASD FieldSpec handheld spectroradiometer

Raw data is a function of the characteristics of the light field being measured, and of the instrument itself. Reflectance is the actual fraction of incident light that is reflected from a surface, while transmittance is the fraction, which passes through a given material. Radiance ($Wm^{-2}sr^{-1}nm^{-1}$) can be measured with the bare fibre optic (NFOV) or with directional foreoptics, such as field of view (FOV) limiters. Irradiance ($Wm^{-2}nm^{-1}$) is measured using the remote cosine receptor (RCR), which integrates the light flux from all directions that would be intercepted by a planar surface (FieldSpec user's guide, 1999).

2.3.2 DustTrak Aerosol Monitor 8520

The DustTrak aerosol monitor 8520 (Figure 2.4) provides a real-time measurement based on 90° light scattering laser photometer. The amount of light scatter determines the particle mass concentration (Liu et al., 2002) which is based on a calibration factor.

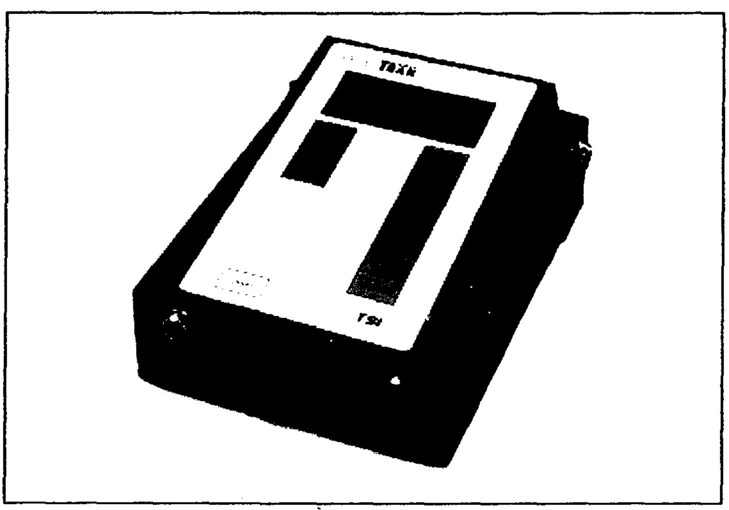

Figure 2.4: DustTrak aerosol monitor 8520

The DustTrak aerosol monitor measures aerosols in a wide variety of environments provides reliable exposure assessment by measuring particle concentrations corresponding to PM1.0, PM2.5, PM10 or respirable size fractions (Trust Science Innovation, TSI, 2003). The DustTrak is a portable, battery-operated laser photometer which gives a real-time digital readout with the added benefits of a built-in data logger. The DustTrak detects potential problems with airborne contaminants such as dust, smoke, fumes and mists.

2.3.3 Garmin E-Trek Vista Hcx GPS

The Garmin E-Trek Vista HCx GPS (Figure 2.5) gives a high sensitive receiver which can be used for geocaching and outdoor use such as hiking. GPS receivers take this information and use triangulation to calculate the user's exact location.

Figure 2.5: Garmin E-Trek vista HCX

A GPS receiver must be locked on to the signal of at least three satellites to calculate a two dimension (2D) position (latitude and longitude) and track movement. With four or more satellites in view, the receiver can determine the user's three dimension (3D) position (latitude, longitude and altitude). Once the user's position has been determined, the GPS unit can calculate other information, such as speed, bearing, track, trip distance, distance to destination, sunrise and sunset time and more (E-Trex HC series owner's manual, 2007).

2.4 Processing Software

2.4.1 PCI Geomatica 10.1

All image processing processes such as geometric and distortion correction, cloud masking, radiometric calibration, atmospheric correction, generating colour-coded maps using developed algorithm and colour-coded classifications were done using Geomatica 10.1. PCI Geomatica 10.1 is an image-centric application that brings together remote sensing, the geographic information system (GIS), cartography and photogrammetry into an integrated environment.

2.4.2 Atmospheric/Topographic Correction (ATCOR)

The algorithm used for haze removal atmospheric and topographic correction, (ATCOR) developed originally by Richter (Richter, 1996a, 1996b, 1997, 2005; Richter et al., 2009). For processing, two variants are selectable: the ATCOR2 allows a 2D atmospheric correction, and the ATCOR3 that permits for an additional 3D topographic correction including the use for a digital elevation model (DEM). Furthermore, a version for the correction of air-borne sensors is available in ATCOR4, which additionally takes the scanning angle into account.

Atmospheric correction permits the correction of optical remote sensing imagery in the spectral range between 0.4 and 2.5 µm as well as in the thermal range between 8 and 14 µm. It is convenient for the imagery of Landsat, Satellite Pour Observation de la Terre (SPOT), Indian Remote Sensing Satellite (IRS), Advanced

Spaceborne Thermal Emission and Reflection Radiometer (ASTER), IKONOS and QuickBird. The software uses a data base which rests upon the MODerate spectral resolution atmospheric TRansmittance algorithm (MODTRAN 4) code for the radiative transfer from measured digital numbers to the radiance at the sensor.

The clear image areas (around 40 %) are needed beneath hazy parts for the application of ATCOR announced by Geosystems (2009, 2010). Only hazy areas could be corrected but not clouds which make the surface invisible completely. The blue and red image bands must have a high correlation to achieve good results. If the blue band is missing the correction is still possible but leads to non-perfect results. The algorithm is not suitable for haze over water; this will result to more noise in such areas.

2.4.3 FieldSpec RS3

The FieldSpec RS3 software is designed with a graphical user interface (GUI) that provides simplicity for the data collection. It is pre-installed on the computer accompanying the ASD FieldSpec handheld spectroradiometer instrument for taking measurements. This software, running with the colour liquid crystal display (LCD), can be run in high contrast (black and white) for better visibility outdoors over bright sunlight. The main use of this software is to record spectroradiometer measurements in terms of the DN, reflectance, radiance and irradiance. The data recorded by using RS3 can be interpreted by using the ASD view spec pro software.

2.4.4 ASD View Spec Pro

The ASD view spec pro was used to open and read all data that has been saved by RS3 software in .exe format. The saved data can be analysed through this software and saved either in RS3.exe or exported to Microsoft Excel format.

2.4.5 Minitab and Excel Statistical Software

The statistical analysis was performed using Minitab and Excel Statistical Software. All statistical analyses such as plotting the graph, calculating the correlation coefficient (R) and the root mean square error (RMSE) for each regression analysis and algorithm validation accuracy analysis were done using this software.

2.5 Satellite Data

2.5.1 Land Observing Satellite (LANDSAT)

The Landsat has been one of the primary operational earth observation satellites over the past three decades. With the long-term historical image records and the high spatial resolution of 30 x 30 m in the short wave bands and 60–120 m in the thermal band, the Landsat thematic mapper (TM) and enhanced thematic mapper plus (ETM+) images have been widely utilised for both research and non-research purposes.

The newest in this series of remote sensing satellites is Landsat 7 ETM+ which was launched on 15 April 1999. Landsat 7 has the new Enhanced Thematic Mapper Plus (ETM+) sensor. This sensor has the same 7 spectral bands as its predecessor TM, but has an added panchromatic band with 15 m resolution and a lower